Int. J. Electrochem. Sci., 12 **(2017)** 5553 – 5566, doi: 10.20964/2017.06.33

International Journal of
ELECTROCHEMICAL
SCIENCE
www.electrochemsci.org

Inhibitive Effect of L-Lysine on the Corrosion of Mild Steel in Acidic Solutions

Xingwen Zheng[1,2,*], *Min Gong*[2], *Chuan Liu*[2]

[1] School of Chemical and Environmental Engineering, Sichuan University of Science & Engineering, Zigong 643000, China
[2] Key Laboratory of Material Corrosion and Protection of Sichuan Province, Zigong 643000, China
[*]E-mail: zxwasd@126.com

Received: 5 February 2017 / *Accepted:* 11 April 2017 / *Published:* 12 May 2017

The inhibition performance and mechanism of L-lysine for the corrosion of mild steel in acidic solutions were investigated using electrochemical measurements and Quantum chemical calculation. The results revealed that L-lysine acted as a mixed-type inhibitor with a predominantly cathodic action for mild steel in 1 M HCl solution, but as a modest cathodic inhibitor for mild steel in 0.5 M H_2SO_4 solution. The adsorption of L-lysine on steel surface obeyed Langmuir adsorption isotherm, and the thermodynamic parameters were further determined based on the model. Moreover, quantum chemical calculation gave further insight into the mechanism of inhibition of L-lysine. Besides, the synergistic inhibition effect of L-lysine and chloride ion was also observed for the corrosion of mild steel.

Keywords: Mild steel; L-lysine; Acidic solutions; Adsorption isotherm; Quantum chemical calculation.

1. INTRODUCTION

Organic inhibitors are commonly used to inhibit the corrosion of metals in aggressive media, especially in acidic solutions. However, most of organic inhibitors are synthetic chemicals, expensive and very hazardous to both human health and the environment, thus, the development of non-toxic or low-toxic inhibitors has received much attention in current research [1-5]. Thereinto, amino acids are known to be a kind of effective non-toxic inhibitor for metallic materials in corrosive media [1,6-12]. Bobina and co-workers reported the inhibitory properties of L-histidine on the corrosion of carbon steel in weak acid media containing acetic acid/sodium acetate [11]. Mendonça et al. evaluated six amino acids as corrosion inhibitors for carbon steel and copper in 0.5 M H_2SO_4 solution through electrochemical techniques and theory computations [9]. Some amino acids as inhibitors for copper

corrosion in 8 M phosphoric acid at different temperatures were investigated [1]. And, the synergistic inhibition effect of imidazoline derivative and L-cysteine on carbon steel corrosion in a CO_2-saturated brine solution was studied by Zhao's research group [12]. Moreover, the corrosion inhibition of amino acid derivatives such as amino acid-derived ionic liquid [13], Schiff's bases [14,15] and nonionic surfactants [16] was also researched. L-lysine is a basic amino acid, containing two amino groups and a carboxyl group, which could be seemed as an effective potential inhibitor. And the results have been shown that organic inhibitors exhibit different corrosion inhibition performance in different acid solutions [17,18], but there are few reports on amino acids in this field. In present work, electrochemical techniques are employed to investigate the inhibition effect of L-lysine on the corrosion of mild steel in 1 M HCl solution and 0.5 M H_2SO_4 solution, respectively. Moreover, the inhibition mechanism of L-lysine and the influence of chloride ion on the inhibitory effect of L-lysine are also discussed.

2. EXPERIMENTAL

2.1. Electrolyte and Material

The 0.5 M H_2SO_4 and 1 M HCl solutions were prepared using distilled water with analytical grade sulphuric acid and hydrochloric acid, respectively. L-lysine was purchased from Shanghai Ru Ji Biological Technology Development Co. Ltd. The chemical composition (in wt%) of mild steel as follows: C (0.16%), Si (0.18%), Mn (0.29%), P (0.014%), S (0.013%) and Fe for balance. The steel sample was cut into 10 mm × 5 mm with an exposed surface area of 0.785 cm^2, while the remainder was embedded by epoxy. Prior to experiments, the sample was grinded by SiC abrasive paper (200,400, 600 and 800 grade), then rinsed with distilled water, degreased in acetone and dried at room temperature.

2.2. Electrochemical Measurements

Electrochemical experiments were conducted through the conventional three-electrode system using CHI660E electrochemical workstation (Shanghai Chenhua Instrument Co. Ltd.), in which the auxiliary electrode and reference electrode was the platinum electrode and saturated calomel electrode (SCE), respectively. In the experiments, the solution temperature was controlled by a constant temperature water bath with an accuracy of 1 K, and the electrolytic cell was open to the air and under a static condition.

Before measuring electrochemical impedance spectroscopy (EIS), the open circuit potential (OCP) of steel electrode in test solution was monitored for 30 minutes, then the electrochemical impedance spectroscopy was measured using AC signals 5 mV peak to peak in the frequency range from 10^{-2} Hz to 10^5 Hz. At last, the polarization curve was obtained by potentiodynamic scanning method in the potential range from -250 to +250 mV relative to OCP with a scan rate of 0.5 mV/s.

2.3. Quantum Chemical Calculations

Quantum chemical calculation was conducted through Gaussian G09 program using the B3LYP method of density functional theory (DFT) at the basis set level of 6-311++G(d,p). The molecular structure of L-lysine was geometrically optimized, and related quantum chemical parameters, including the energy of the highest occupied molecular orbital (E_{HOMO}), the energy of the lowest unoccupied molecular orbital (E_{LUMO}), energy gap ($\Delta E = E_{LUMO} - E_{HOMO}$), fraction of electrons transferred (ΔN) and dipole moment (μ), were calculated.

3. RESULTS AND DISCUSSION

3.1. OCP-Time Curves

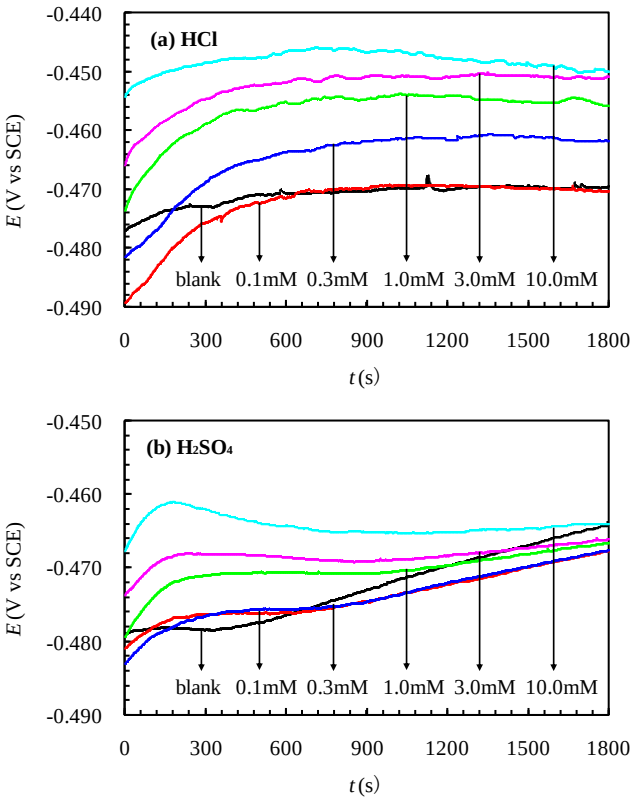

Figure 1. OCP-time curves of mild steel in 1 M HCl (a) and 0.5 M H_2SO_4 (b) solutions without and with different concentrations of L-lysine at 298 K.

The variation of the open circuit potential of steel electrode with time in the test solution is presented in Figure 1. Figure 1(a) shows the OCP of mild steel in HCl solution increases gradually and finally approaches to a steady state, and the OCP value increases with the increase in the concentration of L-lysine, which indicate that L-lysine may influence the anodic reaction of mild steel in HCl solution [19-20]. However, the OCP of mild steel in H_2SO_4 solution, as shown in Figure 1(b), is continuously increasing until the concentration of corrosion inhibitor higher than 3.0 mM, but the addition of L-lysine reduces the growth rate of potential. A more negative OCP observed in the

absence of L-lysine indicates that L-lysine has influenced the cathodic reaction of mild steel in H_2SO_4 solution [19-20]. Obviously, the different change trends of OCP reflect the differences in corrosion mechanism of mild steel in two kinds of acid solutions.

3.2. Potentiodynamic Polarization Curves

Figure 2(a) shows the potentiodynamic polarization curves for mild steel in 1 M HCl solution without and with different concentrations of L-lysine at 298 K, from which it can be clearly seen that adding L-lysine leads to the anodic branch and cathodic branch of the polarization curves shift to the direction of low current density, and the current density decreases with increasing inhibitor concentration, which indicate that L-lysine inhibits both the anodic dissolution of mild steel and the cathodic reduction of hydrogen ions, but obviously the inhibitory effect of L-lysine on the cathode reaction is greater than that on the anode reaction. Moreover, there is obvious Tafel region in the polarization curves. Thus, the related electrochemical parameters such as corrosion potential (E_{corr}), corrosion current density (I_{corr}), and Tafel slopes of anode (β_a) and cathode (β_c) are determined by Tafel extrapolation [21-23], and are listed in Table 1. Subsequently, the inhibition efficiency (η) is calculated by the following equation [22-23]:

$$\eta(\%) = (1 - \frac{I_{corr}}{I_{corr,0}}) \times 100 \qquad (1)$$

where, $I_{corr,0}$ and I_{corr} is the corrosion current density of mild steel electrode in the uninhibited and inhibited solutions, respectively.

However, the polarization curves of mild steel in 0.5 M H_2SO_4 solution, as shown in Figure 2(b), display that the cathodic reaction of the corrosion of mild steel is inhibited when L-lysine is added to the H_2SO_4 solution, and the inhibition increases with the increase of inhibitor concentration, but the anodic polarization curves almost overlap together and do not exist the Tafel linear region, therefore, the electrochemical parameters are determined by Tafel extrapolation of the cathodic polarization curves to the E_{corr} [24], and are listed in Table 1.

Table 1 illustrates that the value of I_{corr} decreases, accordingly, the inhibition efficiency (η) is improved, when the L-lysine concentration is increased, and the inhibitive effect of L-lysine on the corrosion of mild steel in HCl solution is better than that in H_2SO_4 solution. Meanwhile, the values of E_{corr} do not change significantly, although the E_{corr} of steel electrode in 0.5 M H_2SO_4 solution becomes more negative with the incremental inhibitor concentration, but the displacement is less than 20 mV. Moreover, considering the values of β_a and β_c are slightly changed, it can be thought that the presence of L-lysine has little influence on the corrosion mechanism of mild steel in the test solutions, namely, the inhibition of L-lysine is based on the geometric blocking effect [18,25]. As suggested above, L-lysine can be seen as a mixed-type inhibitor with a predominantly cathodic action for mild steel in HCl solution [26], but a modest cathodic inhibitor for mild steel in H_2SO_4 solution [27].

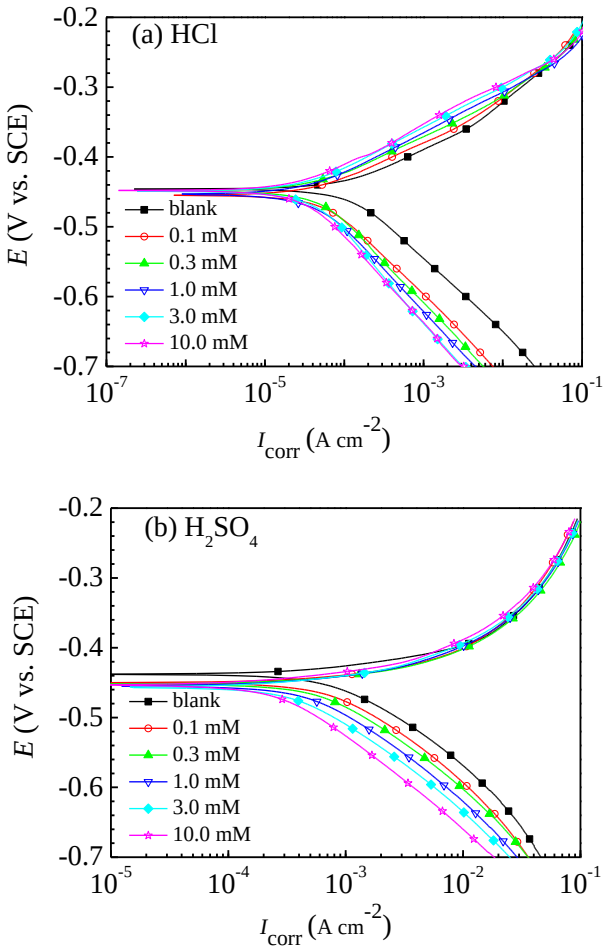

Figure 2. Potentiodynamic polarization curves of mild steel in 1 M HCl (a) and 0.5 M H_2SO_4 (b) solutions without and with different concentrations of L-lysine at 298 K.

Table 1. The electrochemical parameters for mild steel in 1 M HCl and 0.5 M H_2SO_4 solution without and with different concentrations of L-lysine at 298 K.

System	C(mM)	E_{corr} (V vs. SCE)	I_{corr}(mA cm^{-2})	β_a(mV dec^{-1})	-β_c(mV dec^{-1})	η(%)
1 M HCl	blank	-0.446	0.117	55.0	103.4	\
	0.1	-0.448	0.065	53.5	101.3	43.8
	0.3	-0.448	0.047	54.1	123.4	60.0
	1.0	-0.453	0.040	59.4	120.1	65.8
	3.0	-0.449	0.039	59.3	135.9	66.3
	10.0	-0.448	0.035	66.1	124.4	70.2
0.5M H_2SO_4	blank	-0.438	0.853	\	119.4	\
	0.0001	-0.450	0.766	\	123.8	10.3
	0.0003	-0.452	0.608	\	119.5	28.7
	0.001	-0.455	0.491	\	120.4	42.5
	0.003	-0.456	0.356	\	116.4	58.2
	0.01	-0.458	0.312	\	121.9	63.4

3.3. Electrochemical Impedance Spectroscopy (EIS)

Figures 3 and 4 show the Nyquist (a) and Bode (b) plots of mild steel obtained in 1 M HCl and 0.5 M H_2SO_4 solutions without and with different concentrations of L-lysine at 298 K, respectively. It can be seen from Figures 3(a) and 4(a) that the addition of L-lysine has little influence on the shapes of Nyquist plots, except that the diameter of capacitive loop signficantly enhances with the increase in L-lysine concentration, which suggest the presence of L-lysine dose not change the corrosion mechanism of mild steel in test solutions [28-29], and that is consistent with the analytical results of polarization curves. Nyquist plots in Figure 3(a) show a depressed capacitive loop due to the roughness and inhomogeneity of electrode surface [2,30], but in Figure 4(a) is composed of a capacitive loop at high frequencies (HF) and an inductive loop at low frequencies (LF), which may reflect the difference of corrosion mechanism of mild steel in HCl and H_2SO_4 solutions. The capacitive loop is usually considered to correspond to the time constant of charge transfer and double layer capacitance (C_{dl}) [31], while the LF inductive loop may be attributed to the relaxation process caused by adsorption species such as $(SO_4^{2-})_{ads}$ and $(H^+)_{ads}$ on the electrode surface [2,32-33]. Figures 3(b) and 4(b) show the values of phase angle and impedance magnitude (|Z|) increase with the increasing of L-lysine concentration, which indicate better protection of inhibitor with higher concentrations [22].

Based on the above mentioned discussion and description, the impedance parameters are obtained by fitting the EIS to the equivalent circuits as shown in Figure 5 using ZSimpWin software, and are given in Table 2. In the circuits, R_S is the resistance of solution, L and R_L represent the inductive element and inductive resistance, respectively. R_{ct} is the charge transfer resistance, and due to the imperfections of the surface, constant phase element (CPE) is usually used to replace double layer capacitance (C_{dl}) [34-35], and CPE can be described as follows [34,36]:

$$Z_{CPE} = \frac{1}{Y_0 (j\omega)^n} \quad (2)$$

where Y_0 is the CPE constant, j is the imaginary unit, ω is the angular frequency, and n is the deviation parameter, which is often related to the surface morphology. The C_{dl} value and inhibition efficiency (η) is respectively calculated according to the following equations [30,33]:

$$C_{dl} = Y_0 (\omega_{max})^{n-1} = Y_0 (2\pi f_{Z\,im\text{-}max})^{n-1} \quad (3)$$

$$\eta = \frac{R_{ct} - R_{ct,0}}{R_{ct}} \times 100 \quad (4)$$

where, $R_{ct,0}$ and R_{ct} is the charge transfer resistance without and with inhibitor, respectively.

Table 2 shows that the R_{ct} values increase, and the values of C_{dl} decrease with increasing L-lysine concentration, correspondingly, the inhibition efficiencies go up, which are attributed to the increase of surface coverage caused by the L-lysine adsorption on the mild steel surface [37-38]. The value of n is close to one, indicating the charge transfer process controls the dissolution mechanism of mild steel in test solution [37-38]. And, the inhibition efficiencies are in good agreement with those obtained from polarization curves. In addition, the inhibition efficiency of L-lysine is compared with that of other amino acids reported in literature [9,39], the related data are listed in Table 3. It can be seen that the inhibition efficiency of L-lysine is slightly less than that of two sulfur amino acids (L-cysteine and L-methionine) in 0.5 M H_2SO_4 solution, but higher than that of containing amide group

amino acids (L-glutamine and L-asparagine) and another basic amino acid L-arginine. However, in 1 M HCl solution, L-lysine exhibits good inhibition property, its inhibition efficiency is higher than that of L-cysteine and hydroxyl containing L-serine, but still below that of L-tryptophan and L-histidine, which may be attributed to the nitrogen heterocyclic ring in their molecules.

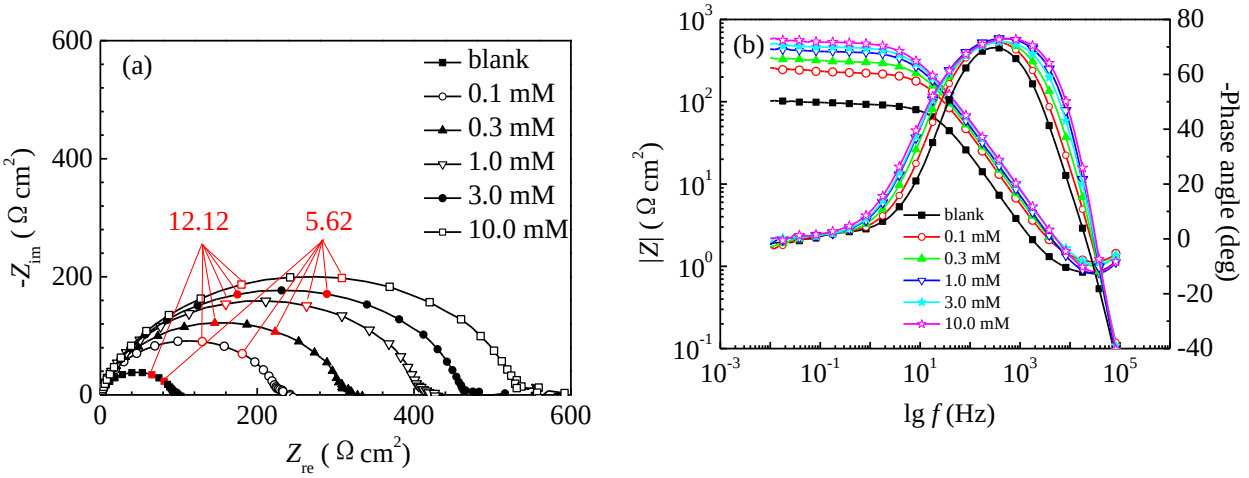

Figure 3. Nyquist plots (a) and Bode plots (b) for mild steel in 1 M HCl solution without and with different concentrations of L-lysine at 298 K.

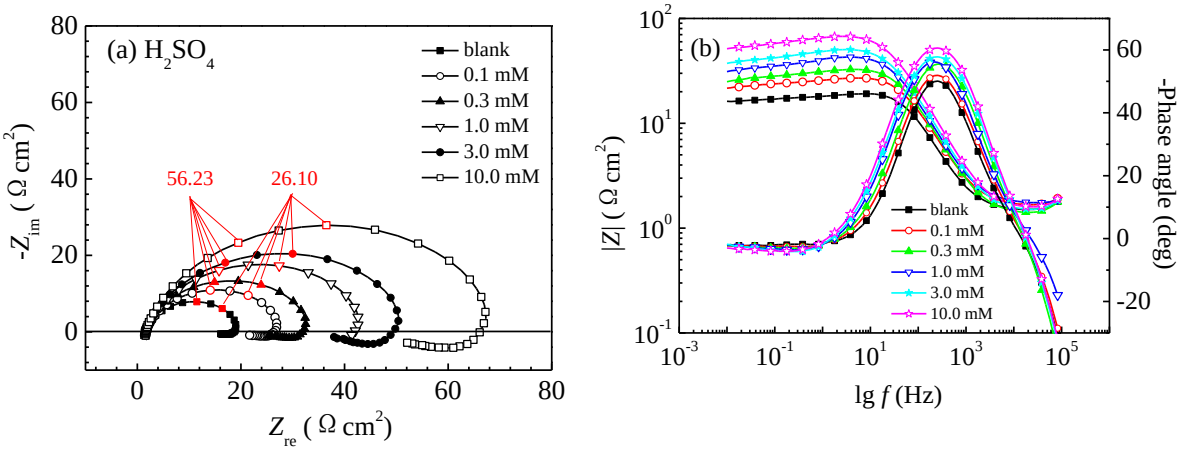

Figure 4. Nyquist plots (a) and Bode plots (b) for mild steel in 0.5 M H_2SO_4 solution without and with different concentrations of L-lysine at 298 K.

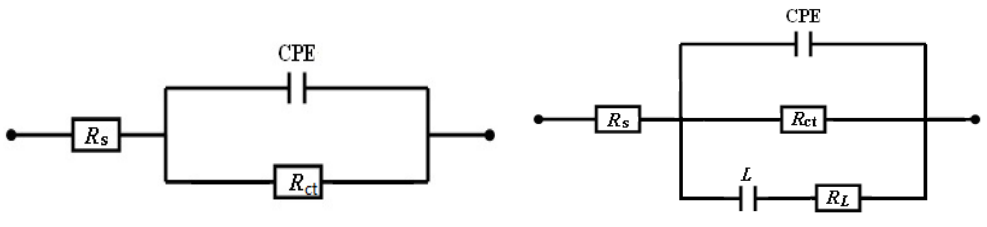

(a) without inductive loop (b) with inductive loop

Figure 5. Equivalent circuits used to fit the EIS without (a) and with (b) inductive loop.

Table 2. The EIS parameters for mild steel in test acid solutions without and with different concentrations of L-lysine at 298 K.

System	C (mM)	R_S (Ω cm^2)	$Y_0\times10^{-6}$ (S s^n cm^{-2})	n	R_{ct} (Ω cm^2)	C_{dl} (μF cm^{-2})	L (Ω cm^2)	R_L (Ω cm^2)	η (%)
1 M HCl	blank	0.5	155.9	0.87	96	82.0	\	\	\
	0.1	1.3	69.8	0.91	229	45.8	\	\	58.1
	0.3	1.2	67.0	0.90	311	42.7	\	\	69.1
	1.0	1.0	61.6	0.89	406	40.6	\	\	76.4
	3.0	1.2	60.5	0.88	459	37.8	\	\	79.1
	10.0	1.0	57.3	0.88	527	36.9	\	\	81.8
0.5 M H_2SO_4	blank	1.6	217.6	0.92	17.7	133.1	26	109	\
	0.1	1.8	205.6	0.89	25.5	113.0	50	129	30.6
	0.3	1.6	182.0	0.90	31.0	105.9	79	142	42.9
	1.0	1.8	203.7	0.88	42.0	103.7	60	140	57.9
	3.0	1.6	182.4	0.88	49.3	95.6	107	178	64.1
	10.0	1.7	147.7	0.89	66.2	82.4	204	257	73.3

Table 3. The inhibition efficiencies obtained from EIS at amino acid concentration of 10.0 mM.

Medium	Amino acid	η(%)	Material	Temperature	Reference
1 M HCl	L-lysine	81.8	mild steel, described in Section 2.1	25 ℃	\
	L-cysteine	80.5	mild steel with composition (wt%) of C(0.18), Mn(0.64), P(0.05), S(0.06) and Fe balance	25 ℃	[39]
	L-serine	47.6			
	L-tryptophan	94.1			
	L-histidine	90.3			
0.5 M H_2SO_4	L-lysine	73.3	mild steel, described in Section 2.1	25 ℃	\
	L-cysteine	81.5	carbon steel, the component not stated	at room temperature (≌ 25 ℃)	[9]
	L-serine	72.6			
	L-methionine	85.9			
	L-asparagine	61.2			
	L-glutamine	53.1			
	L-arginine	43.2			

3.4. Adsorption Isotherm

It is well known that the corrosion inhibition effect of organic molecules is determined by their adsorption on the metal surface [40], while the adsorption isotherm can provide important information on the interaction between the inhibitor and the metal surface. In this study, the adsorption of L-lysine is found to obey the Langmuir adsorption isotherm. Langmuir isotherm can be described by equation 5 [41], in which, C is the concentration of L-lysine, K_{ads} is the adsorption equilibrium constant, θ is the surface coverage, its value is determined by the ratio η /100.

$$\frac{C}{\theta} = C + \frac{1}{K_{ads}} \quad (5)$$

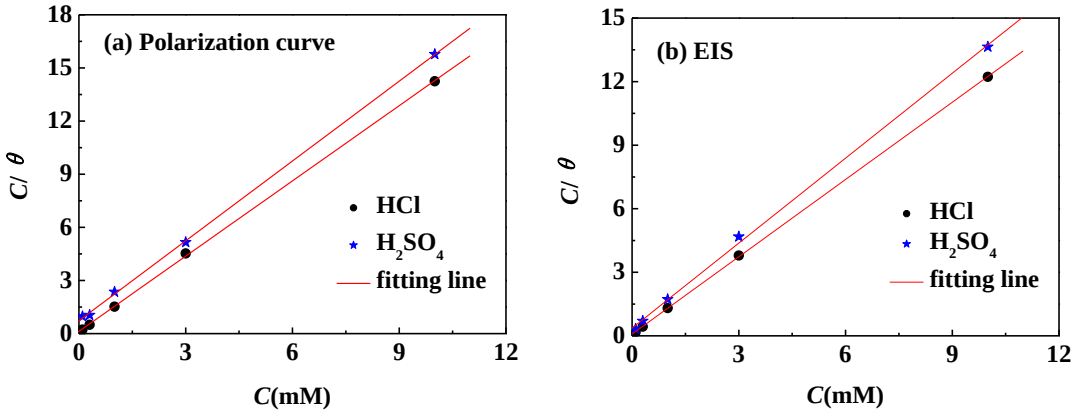

Figure 6. Langmuir isotherm plots for mild steel in acid solutions with different concentrations of L-lysine at 298 K.

Figure 6 shows the plots of C/θ as function of C yield a straight line, and the correlation coefficients (R^2) are greater than 0.998. Then, the value of K_a is obtained from the intercept of the fitting straight line, and the corresponding standard free energy of adsorption process is calculated by the following equation:

$$K_{ads} = \frac{1}{55.5}\exp(-\frac{\Delta G^{\Theta}_{ads}}{RT}) \quad (6)$$

where, R is the universal gas constant T is the thermodynamic temperature, and the value of 55.5 is the molar concentration of water in test solution.

Table 4 shows the values of K_{ads} are relatively large, and the values of ΔG^{Θ}_{ads} are negative, which indicate there is a strong interaction between L-lysine and the steel surface, and the adsorption process is spontaneous. Moreover, it is also noted the K_{ads} value as well as the absolute value of ΔG^{Θ}_{ads} in HCl solution is greater than that in H_2SO_4 solution, which reflect the adsorption affinity of L-lysine onto the mild steel surface in HCl solution is stronger, and thus L-lysine exhibits a better inhibitive performance in HCl solution.

Table 4. The adsorption parameters for mild steel in acid solutions with different concentrations of L-lysine at 298K.

System	Polarization curve		EIS	
	K_{ads}(L/mol)	ΔG^{Θ}_{ads} (kJ/mol)	K_{ads}(L/mol)	ΔG^{Θ}_{ads} (kJ/mol)
1 M HCl	7.99×10^3	-32.21	1.18×10^4	-33.17
0.5 M H_2SO_4	1.36×10^3	-27.84	2.74×10^3	-29.56

3.5. Theoretical Calculation

The optimized geometric structure and the distributions of electrostatic potential, HOMO and LUMO of L-lysine obtained from quantum chemistry calculation through Gaussian 09 software are shown in Figure 7, and the calculated quantum chemical parameters are given in Table 5. As shown in

Figures 7(c) and 7(d), the electron density distributions of frontier molecular orbital of L-lysine are located on the amino group (-NH_2) and the carboxyl group (-COOH), suggesting that N atom and O atom are the active adsorption sites of L-lysine molecule, this also can be confirmed by the distribution of electrostatic potential shown in Figure 7(b). Based on the E_{HOMO} and E_{LUMO}, the value of ΔN calculated by equation 7-9 [42] is greater than zero, which indicates that L-lysine molecule can donate electrons to mild steel surface promoting the formation of adsorptive bonds. While, the HOMO of molecule is often associated with the electron donating ability, and considering the distribution of HOMO in Figure 7(c), therefore, L-lysine is more likely to adsorb on the surface of mild steel by the amino group, especially the amino group at the end of L-lysine. Moreover, the value of μ of L-lysine molecule is higher than that of H_2O [43], due to the dipole-dipole interaction between molecules and metal surface, the L-lysine molecules can replace the water molecules adsorbed on the mild steel surface, and then play a role in inhibition the corrosion of mild steel.

$$\chi = \frac{I + A}{2} \quad (7)$$

$$\gamma = \frac{I - A}{2} \quad (8)$$

$$\Delta N = \frac{\chi_{Fe} - \chi_{inhibitor}}{2(\gamma_{Fe} + \gamma_{inhibitor})} \quad (9)$$

where, I is the ionization potential, A is the electron affinity, and they are defined as $I = -E_{HOMO}$ and $A = -E_{LUMO}$. χ is the absolute electronegativity, and γ is the global hardness. According to the literature [42,44], the theoretical values of χ_{Fe} and γ_{Fe} are 7 eV and 0 eV, respectively.

3.6. Inhibition Mechanism of L-lysine and Its Synergistic Effect with Chlorine Ion

Generally, the inhibition mechanism of organic molecules on the corrosion of metal in acid solution is based on the adsorption of molecules on the metal surface. In acid medium, the protonated L-lysine molecules can directly adsorb on the cathodic sites of the surface of mild steel and decrease the reaction rate of cathodic hydrogen reduction. However, the protonation makes the adsorption of L-lysine on the anodic sites of the mild steel surface become difficult, and previous studies have demonstrated that the steel surface charges positive charge in acid solution [45-46]. But, the surface charge could be changed by the specific adsorption of the anion such as chloride ion (Cl^-), then resulting in the joint adsorption of the anion with the protonated inhibitor molecule [47], while the specific adsorption of sulfate ions (SO_4^{2-}) on the steel surface rarely occur. Thus, the cathodic reaction as well as the anodic reaction of mild steel in HCl solution is inhibited by L-lysine, but L-lysine only inhibits the cathodic reaction of mild steel in H_2SO_4 solution. As a result, the inhibition performance of L-lysine on the corrosion of mild steel in HCl solution is better than that in H_2SO_4 solution.

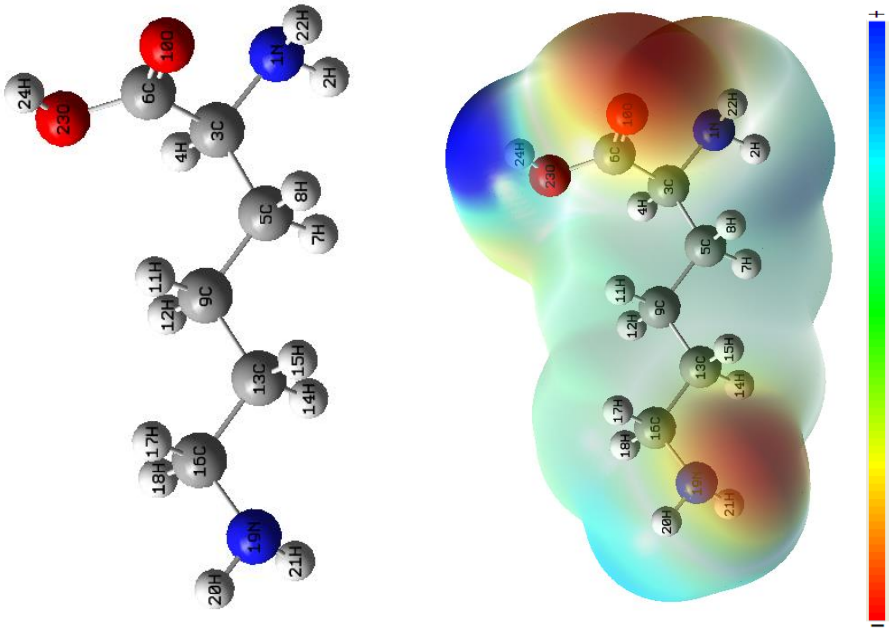

(a) optimized geometric structure (b) distribution of electrostatic potential

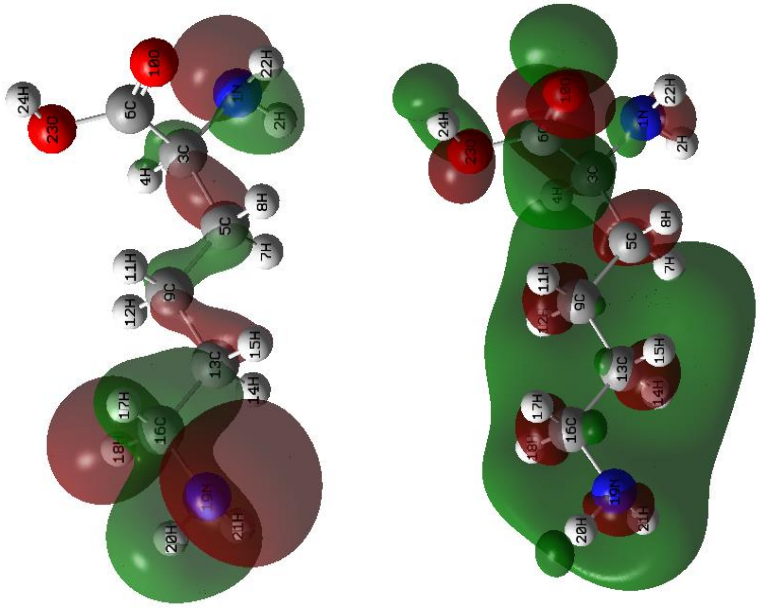

(c) distribution of HOMO (d) distribution of LUMO

Figure 7. The optimized geometric structure (a) and the distribution of electrostatic potential HOMO (b) and LUMO (c) of L-lysine.

Table 5. The quantum chemistry parameters of L-lysine.

E_{HOMO}(eV)	E_{LUMO}(eV)	ΔE(eV)	μ(D)	ΔN
-6.70	-0.44	6.26	2.93	0.55

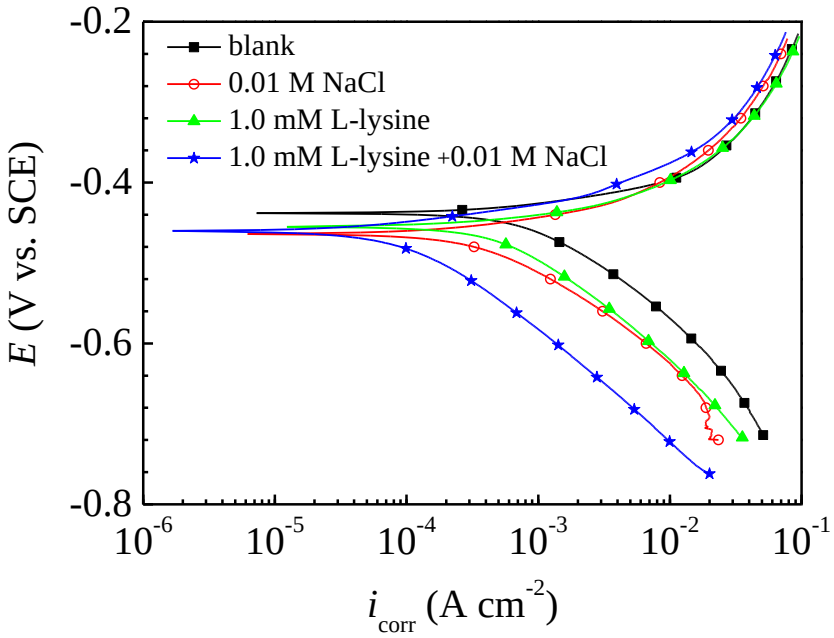

Figure 8. Polarization curves for mild steel in different test solutions at 298 K.

Table 5. The electrochemical parameters for mild steel in different test solutions at 298 K.

System	E_{corr} (V vs. SCE)	I_{corr}(mA cm^{-2})	-β_c(mV dec^{-1})	η(%)	S
blank	-0.438	0.853	119.4	\	\
0.01 M NaCl	-0.464	0.389	107.4	54.4	\
1.0 mM L-lysine	-0.455	0.491	120.4	42.5	\
1.0 mM L-lysine+0.01 M NaCl	-0.460	0.096	120.0	88.7	2.32

Furthermore, in order to confirm the specific adsorption of Cl^-, the effect of chloride ions on the corrosion of mild steel in H_2SO_4 solution and its effect on the corrosion inhibition of L-lysine are determined by potentiodynamic polarization technique, the results show in Figure 8, and the corrosion parameters obtained by Tafel extrapolation method are listed in Table 5. Figure 8 and Table 5 show the addition of sodium chloride (NaCl) mainly inhibits the cathodic reaction of mild steel in H_2SO_4 solution, and has little influence on the anodic reaction. However, when NaCl is added in the H_2SO_4 solution containing L-lysine, although the cathodic reaction is significantly suppressed, the anodic polarization curve is shifted to the direction of low current density, which means that the anodic reaction is inhibited due to the specific adsorption of Cl^-, and the calculated synergies coefficient (S) [33] also indicates that the synergistic inhibitive effect occurs between L-lysine and Cl^- on the corrosion of mild steel in H_2SO_4 solution. Moreover, the nearly parallel anodic polarization curve in Figure 8 illustrates that the addition of NaCl with a concentration of 0.01 M is not enough to change the anodic reaction mechanism of mild steel in the H_2SO_4 solution containing 1.0 mM L-lysine, which is agreement with the research result of Lorenz [48].

4. CONCLUSIONS

Due to the different adsorption capacity of chloride ion and sulfate ion, L-lysine acts as a mixed-type inhibitor with a predominantly cathodic action for mild steel in 1 M HCl solution, but a modest cathodic inhibitor for mild steel in 0.5 M H_2SO_4 solution, and there is synergistic inhibitive effect between L-lysine and Cl^- on the corrosion of mild steel in H_2SO_4 solution. Electrochemical impedance spectroscopy data reveals that the inhibitor molecules adsorb onto the mild steel surface, and the adsorption of L-lysine on the mild steel surface is spontaneous process and obeys the Langmuir adsorption isotherm. Theoretical calculations display the hetero atoms N and O, especially the N atom, are the active adsorption sites of L-lysine.

ACKNOWLEDGEMENTS
This project is supported financially by Talent Project of Sichuan University of Science & Engineering (No. 2016RCL11) and the Opening Project of Key Laboratory of Material Corrosion and Protection of Sichuan Province (No. 2016CL03).

References

1. H.H.A. Rahman, A.H.E. Moustafa and M.K. Awad, *Int. J. Electrochem. Sci*., 7 (2012) 1266.
2. S.N. Victoria, R. Prasad and R. Manivannan, *Int. J. Electrochem. Sci*., 10 (2015) 2220.
3. G. Gece and S. Bilgiç, *Corros. Sci*., 52 (2010) 3435.
4. M.A. Amin, K.F. Khaled, Q. Mohsen and H.A. Arida, *Corros. Sci*., 52 (2010) 1684.
5. A.Y.I. Rubaye, A.A. Abdulwahid, S.B. Al-Baghdadi, A.A. Al-Amiery, A.A.H. Kadhum and A.B. Mohamad, *Int. J. Electrochem. Sci*., 10 (2015) 8200.
6. H. Zhao, X. Zhang, L. Ji, H. Hu and Q. Li, *Corros. Sci*., 83 (2014) 261.
7. K. Barouni, A. Kassale, A. Albourine, O. Jbara, B. Hammouti and L. Bazzi, *J. Mater. Environ. Sci*., 5 (2014) 456.
8. M. Dehdab, M. Shahraki and S.M. Habibi-Khorassani, *Amino Acids*, 48 (2016) 291.
9. G.L.F. Mendonça, S.N. Costa, V.N. Freire, P.N.S. Casciano, A.N. Correia and P.D. Lima-Neto, *Corros. Sci*., 115 (2017) 41.
10. S. Kaya, B. Tüzün, C. Kaya and I.B. Obot, *J. Taiwan Inst. Chem. Eng*., 58 (2016) 528.
11. M. Bobina, A. Kellenberger, J.P. Millet, C. Muntean and N. Vaszilcsin, *Corros. Sci.*, 69 (2013) 389.
12. C. Zhang, H. Duan and J. Zhao, *Corros. Sci.*, 112 (2016) 160.
13. E. Kowsari, S.Y. Arman, M.H. Shahini, H. Zandi, A. Ehsani, R. Naderi, A. PourghasemiHanza and M. Mehdipour, *Corros. Sci.*, 112 (2016) 73.
14. N.K. Gupta, C. Verma, M.A. Quraishi and A.K. Mukherjee, *J. Mol. Liq.*, 215 (2016) 47.
15. H.M.A. El-Lateef, M. Ismael and I.M.A. Mohamed, *Corros. Rev.*, 33 (2015) 77.
16. A.M. Al-Sabagh, N.M. Nasser, O.E. El-Azabawy and A.E. El-Tabey, *J. Mol. Liq.*, 219 (2016) 1078.
17. X. Wang, Y. Wan, Q. Wang and Y. Ma, *Int. J. Electrochem. Sci.*, 8 (2013) 806.
18. X. Li, S. Deng and H. Fu, *Corros. Sci.*, 53 (2011) 302.
19. F.S.D. Souza and A. Spinelli, *Corros. Sci*., 51 (2009) 642.
20. A.A. Al-Alamiery, A.A.H. Kadhum, A.H.M. Alobaidy, A.B. Mohamad and P.S. Hoon, *Materials*, 7 (2014) 662.
21. L. Quej-Aké, A. Contreras and J. Aburto, *Int. J. Electrochem. Sci*., 10 (2015) 1809.

22. A. Singh, A. Gupta, A.K. Rawat, K.R. Ansari, M.A. Quraishi and E.E. Ebenso, *Int. J. Electrochem. Sci.*, 9 (2014) 7614.
23. Q.B. Zhang and Y.X. Hua, *Electrochim. Acta*, 54 (2009) 1881.
24. R. Salghi, D.B. Hmamou, E.E. Ebenso, O. Benali, A. Zarrouk and B. Hammouti, *Int. J. Electrochem. Sci.*, 10 (2015) 259.
25. S. Deng, X. Li and H. Fu, *Corros. Sci*., 53 (2011) 3596.
26. N. Soltani and M. Khayatkashani, *Int. J. Electrochem. Sci*., 10 (2015) 46.
27. S.A. Umoren, Y. Li and F.H. Wang, *Corros. Sci*., 52 (2010) 2422.
28. X. Li, S. Deng, X. Xie and H. Fu, *Corros. Sci*., 87 (2014) 15.
29. H. Gerengi and H.I. Sahin, *Ind. Eng. Chem. Res*., 51 (2012) 780.
30. P. Singh, M.A. Quraishi and E.E. Ebenso, *Int. J. Electrochem. Sci*., 9 (2014) 4900.
31. Y. Qiang, L. Guo, S. Zhang, W. Li, S. Yu and J. Tan, *Sci. Rep.*, 6:33305, DOI: 10.1038/srep33305 (2016).
32. X. Zheng, S. Zhang, W. Li, M. Gong and L. Yin, *Corros. Sci*., 95 (2015) 168.
33. X. Zheng, S. Zhang, M. Gong and W. Li, *Ind. Eng. Chem. Res*., 53 (2014) 16349.
34. J. Tan, L. Guo, T. Lv and S. Zhang, *Int. J. Electrochem. Sci*., 10 (2015) 823.
35. Y. Gonzalez, M.C. Lafont, N. Pebere, G. Chatainier, J. Roy and T. Bouissou, *Corros. Sci.*, 37 (1995) 1823.
36. E.E. Ebenso, M.M. Kabanda, L.C. Murulana, A.K. Singh and S.K. Shukla, *Ind. Eng. Chem. Res*., 51 (2012) 12940.
37. A. Singh, Y. Lin, E.E. Ebenso, W. Liu, K. Deng, J. Pan and B. Huang, *Int. J. Electrochem. Sci*., 9 (2014) 5585.
38. A. Singh, E.E. Ebenso, M.A. Quraishi and Y. Lin, *Int. J. Electrochem. Sci*., 9 (2014) 7495.
39. J. Fu , S. Li, Y. Wang, L. Cao and L. Lu, *J. Mater. Sci*., 45 (2010) 6255.
40. M.M. Kabanda, I.B. Obot and E.E. Ebenso, *Int. J. Electrochem. Sci*., 8 (2013) 10839.
41. Y. Xie, Y. Liu and Z. Yang, *Int. J. Electrochem. Sci*., 10 (2015) 1292.
42. Z. Cao, Y. Tang, H. Cang, J. Xu, G. Lu and W. Jing, *Corros. Sci*., 83 (2014) 292.
43. N.O. Obi-Egbedi and I.B. Obot, *Corros. Sci*., 53 (2011) 263.
44. A.Y. Musa, A.A.H. Kadhum, A.B. Mohamad and M.S. Takriff, *Mater. Chem. Phys*., 129 (2011) 660.
45. X. Li, X. Xie, S. Deng and G. Du, *Corros. Sci.*, 87 (2014) 27.
46. A.K. Singh and M.A. Quraishi, *Corros. Sci*., 53 (2011) 1288.
47. A.M. Abdel-Gaber, B.A. Abd-El-Nabey and M. Saadawy, *Corros. Sci*., 51 (2009) 1038.
48. W.J. Lorenz, *Corros. Sci*., 5 (1965) 121.